J. Fluid Mech. (2006), *vol.* 560, *pp.* 149–158. © 2006 Cambridge University Press
doi:10.1017/S0022112006000759 Printed in the United Kingdom

Spatially localized binary-fluid convection

By ORIOL BATISTE[1], EDGAR KNOBLOCH[2], ARANTXA ALONSO[1] AND ISABEL MERCADER[1]

[1]Departament de Física Aplicada, Universitat Politècnica de Catalunya, Barcelona, Spain

[2]Department of Physics, University of California, Berkeley, CA 94720, USA

(Received 20 March 2006 and in revised form 2 May 2006)

Multiple states of spatially localized steady convection are found in numerical simulations of water–ethanol mixtures in two dimensions. Realistic boundary conditions at the top and bottom are used, with periodic boundary conditions in the horizontal. The states form by a mechanism similar to the pinning region around a Maxwell point in variational systems, but are located in a parameter regime in which the conduction state is overstable. Despite this the localized states can be stable. The properties of the localized states are described in detail, and the mechanism of their destruction with increasing or decreasing Rayleigh number is elucidated. When the Rayleigh number becomes too large the fronts bounding the state at either end unpin and move apart, allowing steady convection to invade the domain. In contrast, when the Rayleigh number is too small the fronts move inwards, and eliminate the localized state which decays into dispersive chaos. Out of this state spatially localized states re-emerge at irregular times before decaying again. Thus an interval of Rayleigh numbers exists that is characterized by relaxation oscillations between localized convection and dispersive chaos.

1. Introduction

Spatially localized states are of great interest in the theory of pattern formation. They occur not only in vibrating granular media (Umbanhowar, Melo & Swinney 1996) and polymeric fluids (Lioubashevski *et al.* 1999), but also in reaction–diffusion systems (Lee *et al.* 1994), nonlinear optics (Vladimirov *et al.* 2002), ferrofluids (Richter & Barashenkov 2005) and in several convection systems, both in two and three dimensions (Spina, Toomre & Knobloch 1998; Blanchflower 1999; Blanchflower & Weiss 2002; Batiste & Knobloch 2005*a*, *b*). Most explanations of the presence of such states refer back to the observation by Fauve & Thual (1990) that the localized states familiar in the subcritical Ginzburg–Landau equation with real coefficients can be stabilized when these coefficients acquire imaginary parts. The resulting theoretical description is natural for systems undergoing overstability, but describes only stable spatially localized states of travelling waves for which the complex Ginzburg–Landau equation is the appropriate amplitude equation. Such states are familiar from both experiments and numerical simulations of binary-fluid convection (Kolodner, Surko & Williams 1989; Steinberg *et al.* 1989; Barten *et al.* 1995; Batiste & Knobloch 2005*a*).

In the present paper we are interested in spatially localized steady states such as those present in magnetoconvection (Blanchflower 1999) and He^3–He^4 mixtures heated from below (Batiste & Knobloch 2005*a*, *b*), and follow Blanchflower (1999) in referring to such states as *convectons* to distinguish them from other localized states

found in binary-fluid convection. Binary-fluid convection offers perhaps the best opportunity for studying states of this type in a laboratory. However, despite progress in visualization at cryogenic temperatures (Woodcraft *et al.* 1999) water–ethanol mixtures provide the most convenient system for such studies. Consequently we focus here on the properties of convectons in water–ethanol mixtures, and use experimentally accessible parameters and boundary conditions to study their properties.

Of particular interest is the fact the convectons are found in a supercritical range of Rayleigh numbers. In this regime the conduction state is unstable to growing oscillations, suggesting that spatially localized states which approach the conduction state at large distances should also be unstable. We find that this suggestion is in fact incorrect, and confirm the suggestion of Spina *et al.* (1998) that localized states can be stable in the supercritical regime for Rayleigh numbers below the onset of absolute instability. We also seek to understand the origin of the convecton states. We show that the convectons can be viewed as bound states of two fronts that connect the conduction state to the convection state; states of this type can be stable as a consequence of the 'pinning' of the fronts to the underlying spatially periodic convection state. The result is the presence of a 'pinning' region in which such states are present. We show, by following the branches of odd- and even-parity convectons, that in the pinning region the convecton branches oscillate back and forth in Rayleigh number, adding a pair of rolls with each oscillation, as they approach the finite-amplitude spatially periodic convection state. This type of behaviour is characteristic of the pinning region as explained in detail by Champneys (1998), Hunt *et al.* (2000) and Coullet, Riera & Tresser (2000), and appears in both variational systems such as the Swift–Hohenberg equation and in non-variational systems such as convection. An extensive bibliography is provided by Burke & Knobloch (2006).

In addition to the origin and stability of the localized states we also examine the fate of these states when the Rayleigh number falls outside the pinning region. We find that if the Rayleigh number is too large the fronts at either end of the convecton 'depin', and start moving apart as new rolls are nucleated pairwise at the edges of the convecton. In this way steady convection invades the conduction state, replacing it by a spatially periodic convection state. In contrast, if the Rayleigh number is reduced below the pinning region the fronts move inwards eroding rolls in a pairwise fashion until the convecton disappears and the system settles into a regime of small-amplitude dispersive chaos (Kolodner, Glazier & Williams 1990; Glazier, Kolodner & Williams 1991). This state is not stable, however, and localized states regrow at irregular times before being eroded again. Thus the convectons are born from a remarkable relaxation oscillation between dispersive chaos and transient localized convection states, as the Rayleigh number is raised beyond the onset of overstability.

2. Formulation of the problem

Binary mixtures are characterized by cross-diffusion quantified by the separation ratio S. When $S<0$ the heavier component (of concentration C) migrates up the temperature gradient. Thus in a layer heated from below the destabilizing temperature gradient competes with a stabilizing concentration gradient that develops in response to the heating. If this effect is strong enough convection sets in as growing oscillations once the Rayleigh number R exceeds a critical value R_c; this instability is typically subcritical and develops into a variety of travelling wave states depending on parameters and initial conditions.

The system is described by the dimensionless equations (Batiste *et al.* 2001)

$$\boldsymbol{u}_t + (\boldsymbol{u}\cdot\nabla)\boldsymbol{u} = -\nabla P + \sigma R[(1+S)\theta - S\eta]\hat{\boldsymbol{z}} + \sigma\nabla^2\boldsymbol{u}, \tag{2.1}$$

$$\theta_t + (\boldsymbol{u}\cdot\nabla)\theta = w + \nabla^2\theta, \tag{2.2}$$

$$\eta_t + (\boldsymbol{u}\cdot\nabla)\eta = \tau\nabla^2\eta + \nabla^2\theta, \tag{2.3}$$

together with the incompressibility condition

$$\nabla\cdot\boldsymbol{u} = 0. \tag{2.4}$$

Here $\boldsymbol{u}\equiv(u, w)$ is the velocity field in (x, z) coordinates, P is the pressure, and θ denotes the departure of the temperature from its conduction profile, in units of the imposed temperature difference $\Delta T = T_1 - T_0 > 0$ across the layer. The variable η is defined such that its gradient represents the dimensionless convective mass flux. Thus $\eta \equiv \theta - \Sigma$, where $C = 1 - z + \Sigma$ is the concentration of the heavier component in units of the concentration difference that develops across the layer as a result of cross-diffusion. The system is specified by four dimensionless parameters: the Rayleigh number R providing a dimensionless measure of the imposed temperature difference ΔT, the separation ratio S that measures the resulting concentration contribution to the buoyancy force due to cross-diffusion, and the Prandtl and Lewis numbers σ, τ, in addition to the aspect ratio Γ. For no-slip fixed-temperature boundaries $\boldsymbol{u} = \theta = \eta_z = 0$ on $z = 0, 1$; periodic boundary conditions are used in the horizontal, with period Γ. In the following we shall be interested in steady solutions of even and odd parity satisfying, respectively, $(u(x, z),\ w(x, z),\ \theta(x, z),\ \eta(x, z)) = (-u(-x, z),\ w(-x, z),\ \theta(-x, z),\ \eta(-x, z))$ and $(u(x, z),\ w(x, z),\ \theta(x, z),\ \eta(x, z)) = -(u(-x, 1-z),\ w(-x, 1-z),\ \theta(-x, 1-z),\ \eta(-x, 1-z))$ relative to a suitable origin in x. These are the only steady solutions that can bifurcate from the conduction state.

Equations (2.1)–(2.4) are solved in two dimensions using a spectral code, with a Fourier expansion in the horizontal and a Chebyshev collocation method in the vertical. For the time evolution a second-order time-splitting algorithm proposed by Hugues & Randriamampianina (1998) is used. Below we describe our results for water-ethanol mixtures with $S = -0.021$, $\sigma = 6.22$, $\tau = 0.009$. These parameter values correspond to those used by Kolodner *et al.* (1990) in their experiments on dispersive chaos, and typically require 30 collocation points in the vertical direction, with a time step $\Delta t = 10^{-3}$ in units of the vertical thermal diffusion time. Most of our calculations were performed with $\Gamma = 60$; for this spatial period 1200 points proved sufficient for the Fourier pseudospectral evaluation. In addition, to calculate steady solutions in an efficient manner we have adapted a pseudo-spectral first-order time-stepping formulation to carry out Newton's method (Mamum & Tuckerman 1995), and implemented a continuation code to follow branches of stationary solutions (Mercader, Batiste & Alonso 2006).

3. Convectons

Figure 1 summarizes the results in the form of a bifurcation diagram. It shows $\bar{N} - 1$ as a function of R where $\bar{N}$ is the (time-averaged) Nusselt number; this quantity provides a dimensionless measure of the strength of convection. Convection sets in at a Hopf bifurcation when $R = R_c \approx 1760.8$ and leads to branches of both travelling waves (TW) and standing waves (SW), both spatially periodic and of uniform amplitude in $0 \leqslant x < \Gamma$. Since the TW branch is subcritical both branches are unstable near $R = R_c$ (Knobloch 1986). The unstable TW branch can be followed numerically by seeking steady solutions to the equations in an appropriately moving frame; the speed of this frame is determined by fixing the phase of the solution (Mercader *et al.* 2006). The same numerical method also determines the branch of steady overturning convection (SOC). The results show that the SOC branch passes though a saddle-node bifurcation at $R \approx 1743.3$, but remains unstable until a parity-breaking bifurcation at

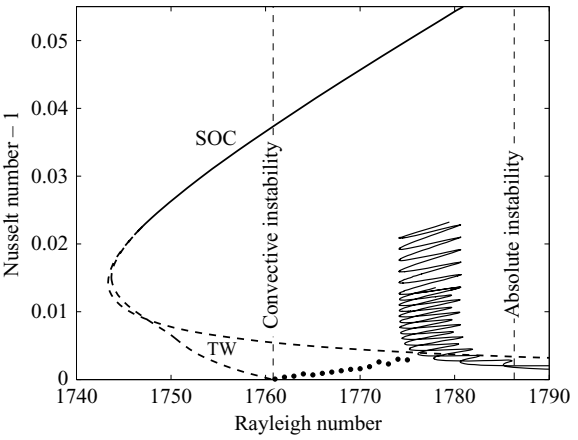

FIGURE 1. Bifurcation diagram showing $\bar{N}$ as a function of the Rayleigh number R when $\Gamma = 60$. The conduction state loses stability at $R_c = 1760.8$. Steady spatially periodic convection (SOC) acquires stability at a parity-breaking bifurcation marking the destruction of a branch of spatially periodic travelling waves (TW). Above threshold small-amplitude dispersive chaos is present (solid dots), which leads into the pinning region ($1774 < R < 1781$) containing a multiplicity of stable localized states of both even and odd parity.

$R \approx 1747.0$ where the TW branch terminates on the SOC branch. In the following it will be important that this point lies below R_c so that there is a large range of stable SOC states that coexist with a stable conduction state ($R < R_c$) and the small-amplitude dispersive chaos state that 'bifurcates' from R_c, apparently supercritically (figure 1).

As R increases beyond R_c the amplitude of the dispersive chaos gradually increases until it begins to be interrupted by episodes in which an almost time-independent spatially localized state emerges. These states grow super-exponentially from the dispersive chaos state, but the saturated state is not stable and is eroded on a much longer time scale; once this erosion is complete dispersive chaos is re-established, but remains 'unstable' to the formation of new localized states, and the process therefore repeats in an irregular fashion (figure 2).

At larger values of R we find steady stable spatially localized states of both odd and even parity (figure 1), and refer to these states as convectons. Figure 3(a) shows the evolution of a small-amplitude initial perturbation into an odd-parity convecton when $R = 1775$, $\Gamma = 60$. In steady state the convecton consists of stationary rolls of uniform amplitude and wavelength, except for two 'front'-like structures at either end that separate it from the void.

Figure 4(a) shows that all odd-parity convectons lie on a connected curve that 'snakes' from small amplitude towards the amplitude of the coexisting spatially periodic roll state, while figure 4(b) shows the corresponding results for even convectons. In each case stable convectons are found on portions of each branch between a left turning point and the next right turning point going up the snake. These turning points correspond to saddle-node bifurcations and hence to change in stability with respect to localized perturbations of the same parity as the convecton. Figure 5 shows sample convecton profiles at or near several turning points on each branch; these indicate that each convecton acquires a pair of rolls between corresponding turning points as one proceeds up each snake. As a result the convectons higher up each snake become broader and broader. On an infinite domain this process proceeds indefinitely as roll pairs are added and the convectons approach an infinitely extended

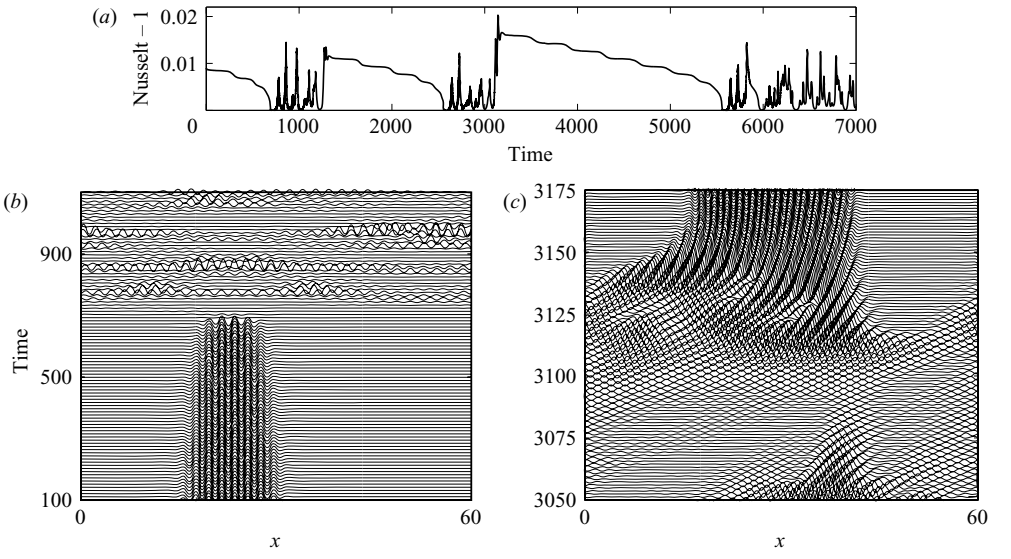

FIGURE 2. (*a*) $N(t)$ at $R = 1774$ showing relaxation oscillations between dispersive chaos and localized steady convection. Space–time plots at two different time intervals in the time series (*a*), showing (*b*) the destruction of localized steady convection, and (*c*) the formation of localized steady convection from dispersive chaos. Time is in units of the thermal diffusion time in the vertical.

SOC state. Note that the turning points at left and right line up exponentially quickly, producing a well-defined pinning region in between.

The structure of the even convectons is greatly influenced by the rolls at either end. A roll rotating clockwise at the right end entrains higher concentration fluid into the convecton, while a counter-clockwise rotating roll entrains lower concentration fluid. Since the addition of a roll pair changes the direction of the outermost rolls its effect manifests itself in the homogenized concentration within the convecton (figure 5*b*). In contrast, the rolls at the ends of an odd-parity convecton always rotate in the same sense, resulting in the entrainment of higher concentration at one end and lower concentration at the other end. The net effect is that the homogenized concentration corresponds to the average concentration (figure 5*a*). It is clear, however, that the net effect of this process is to pump concentration through odd-parity convectons, an effect that manifests itself in the inclination of the concentration contours in the 'conduction' part of odd-parity states (figure 5*a*). Thus all odd-parity states pump flux horizontally.

4. Theoretical interpretation

On an unbounded domain it is appropriate to think of the localized states as homoclinic orbits to the origin, here representing the conduction state (Balmforth 1995). Theory (e.g. Burke & Knobloch 2006) shows that the odd and even localized states bifurcate from the conduction state together with the SOC branch. All three branches bifurcate in the same direction, towards smaller R. The localized states are initially unstable but can be followed using branch-following methods towards lower values of R where they begin to snake towards the SOC state as shown in figure 4(*a*, *b*), and acquire stability. We can understand the origin of this snaking if we think of the SOC as a periodic orbit in eight-dimensional phase space, with x playing the role of time. The localized states then result from visits to the neighbourhood of

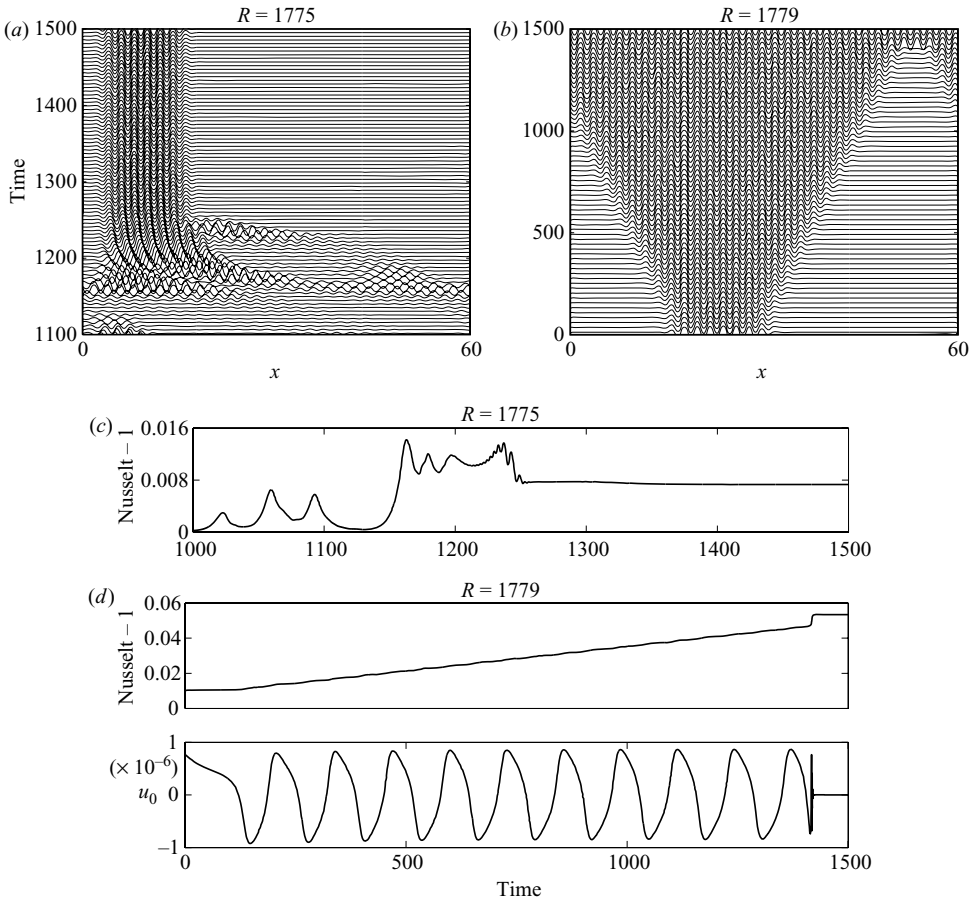

FIGURE 3. (*a*) The formation of an odd parity convecton when $R = 1775$, $\Gamma = 60$ starting from small-amplitude initial conditions, in the form of a space–time plot of $\theta(x, z = 1/2, t)$ with time increasing upward. (*b*) The destruction of this state when R is increased from $R = 1775$ to $R = 1779$. Both fronts advance at the same rate preserving the parity of the state. (*c*) Evolution of N corresponding to (*a*). (*d*) Evolution of N and the zero Fourier mode u_0 of the horizontal velocity corresponding to (*b*).

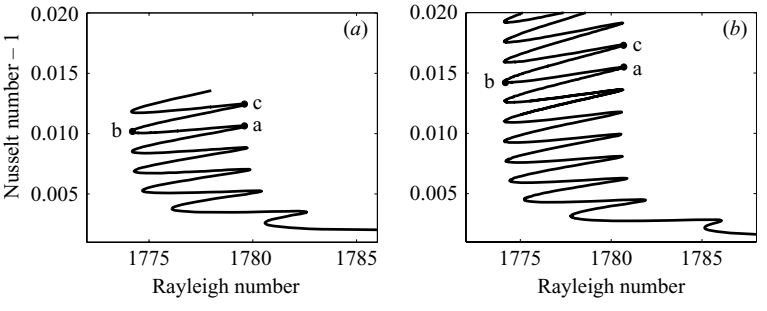

FIGURE 4. Branches of (*a*) odd- and (*b*) even-parity convectons in a $\Gamma = 60$ domain as a function of the Rayleigh number R. Both branches exhibit *snaking*. The convecton profiles at locations labelled a, b, c are shown in figure 5.

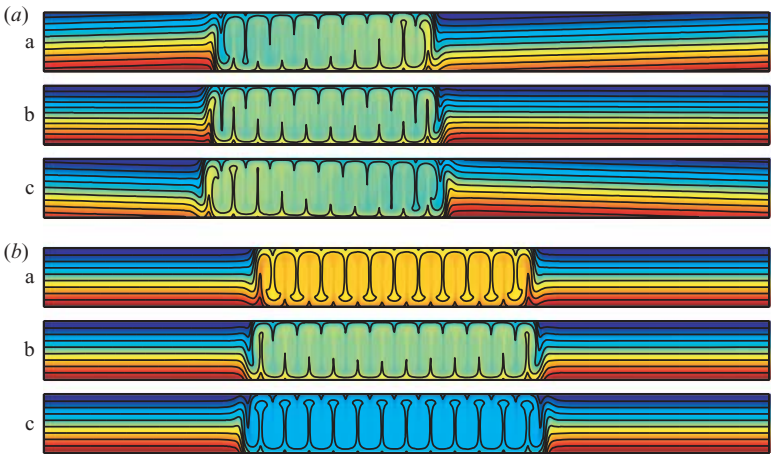

FIGURE 5. Convecton profiles on (*a*) the odd-parity branch, and (*b*) the even-parity branch at the turning points indicated in figure 4(*a*, *b*) in terms of contours of constant C. Each wavelength contains a pair of rolls.

this periodic state; as one proceeds up the snake the spatial trajectory winds around the periodic state more and more before returning to the conduction state, and in the limit results in the formation of a heteroclinic cycle connecting the conduction state to the SOC state and back again. It is possible to show that the snaking is a consequence of this type of phase-space structure (Coullet *et al.* 2000).

It is illuminating, however, to think of the heteroclinic cycle just described in a more physically meaningful way. Here the connection from the conduction state to the SOC state and back again is identified with a pair of fronts separating the conduction state from the SOC state. The convectons are then to be thought of as bound states of these fronts. The origin of the multiplicity of stable convectons and of the associated snaking is easiest to understand in the context of variational systems like the Swift–Hohenberg equation (Champneys 1998; Hunt *et al.* 2000; Coullet *et al.* 2000; Burke & Knobloch 2006). Such systems have a conceptual advantage in having an 'energy' that is a non-increasing function along temporal trajectories. In particular, one can locate parameter values at which pairs of states have identical energy. Such points are called Maxwell points. At a Maxwell point between two spatially homogeneous states fronts connecting such states will be stationary, but for any nearby parameter values such fronts will move, in such a way as to decrease energy. Thus the only stable state away from the Maxwell point is the lower energy state. If, however, one or both states are structured the fronts can be pinned to this structure, resulting in a broadening of the Maxwell point into a pinning region of finite width (Pomeau 1986; Bensimon, Shraiman & Croquette 1988). While the variational structure helps one to focus on the Maxwell point, there is nothing in the above description that requires variational structure *per se*, and indeed it is known that essentially identical behaviour is found in non-variational systems as well provided these are reversible in space, i.e. invariant under $x \to -x$ (Champneys 1998; Hunt *et al.* 2000; Coullet *et al.* 2000). It is for this reason that we refer to the snaking region in figure 1 as the 'pinning' region. Inside this region we have located a multiplicity of distinct but numerically stable coexisting convectons (cf. Batiste & Knobloch 2005*b*). In simpler systems such as the generalized Swift–Hohenberg equation the stable regions are known to be confined between adjacent saddle-node bifurcations, on the portions of the snake extending from a saddle-node bifurcation on the left to the next one on the right going up

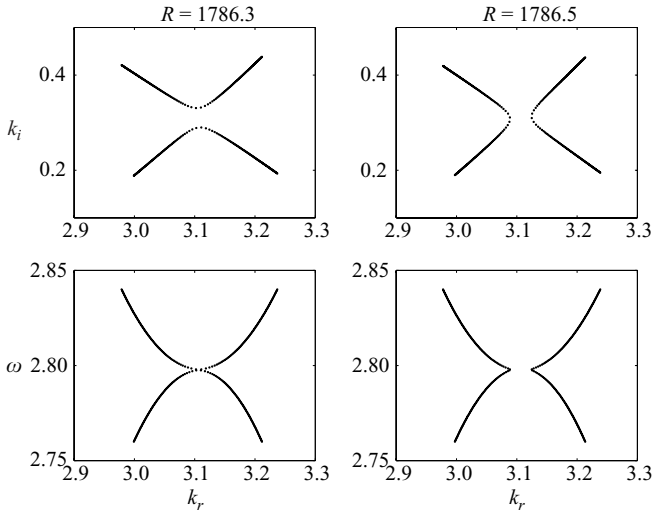

FIGURE 6. Spatial branches of zero growth rate modes in the complex k plane showing the pinching process that occurs at $R = R^* \approx 1786.4$ when $S = -0.021$, $\sigma = 6.22$, $\tau = 0.009$.

each snake (Burke & Knobloch 2006). Our computations are completely consistent with this scenario. On the other hand we have seen no evidence of a change in the wavelength of the rolls comprising a convecton as R varies across the pinning region, in contrast to the Swift–Hohenberg equation.

It is generally believed that a spatially localized state on the real line inherits any instability of the background state, here the conduction state. While this is true in variational problems some care must be taken to interpret this statement correctly when the background is unstable to oscillations. On the real line the Hopf bifurcation at R_c corresponds to the onset of so-called *convective* instability, i.e. for $R > R_c$ small-amplitude localized disturbances do indeed grow, but only in an appropriately moving reference frame, moving with the group velocity. Since near R_c the growth rate is slow, such disturbances are swept either to the left or the right, at least when standing waves are unstable, as in the present case. Only at a larger value of R, hereafter referred to as the absolute instability threshold R^*, does the growth rate exceed the advection rate at the group velocity, and disturbances grow at each fixed x. Spina *et al.* (1998) have argued that under these conditions stable localized states can exist in $R_c < R < R^*$ since in this range the tail of the localized states is only convectively unstable. To confirm this suggestion we have computed R^* for the present problem. This requires the solution of the boundary value problem

$$\begin{pmatrix} \mathrm{i}\omega(\mathrm{D}^2 - k^2) + \sigma(\mathrm{D}^2 - k^2)^2 & \mathrm{i}k\sigma R(1+S) & -\mathrm{i}k\sigma RS \\ \mathrm{i}k & \mathrm{i}\omega + \mathrm{D}^2 - k^2 & 0 \\ 0 & \mathrm{D}^2 - k^2 & \mathrm{i}\omega + \tau(\mathrm{D}^2 - k^2) \end{pmatrix} \begin{pmatrix} \psi \\ \theta \\ \eta \end{pmatrix} = 0, \quad (4.1)$$

$\psi = \mathrm{D}\psi = \theta = \mathrm{D}\eta = 0$ on $z = 0, 1$, obtained from the linearized equations (2.1)–(2.4) by looking for solutions of the form $(\psi, \theta, \eta) = (\psi(z), \theta(z), \eta(z)) \exp(\mathrm{i}kx - \mathrm{i}\omega t)$, where ψ is the streamfunction defined by $\boldsymbol{u} = (\partial_z\psi, -\partial_x\psi)$. Here $\mathrm{D} \equiv \mathrm{d}/\mathrm{d}z$, ω is real but k is taken to be complex. This problem determines the dispersion relation $\omega(k)$ as a function of R. At the absolute instability threshold this relation has a double root $\omega(k)$, subject to a certain pinching condition (Huerre & Monkewitz 1990). This requirement suffices to determine ω, $k \equiv k_r + \mathrm{i}k_i$ and R^*. Figure 6 shows k_i and ω as functions of k_r at $R < R^*$ and $R > R^*$, revealing the pinching process that occurs at

$R = R^*$. Thus at $R^* \approx 1786.4$ the dispersion relation has a double root of the required type; this value will be increased by an $O(\Gamma^{-2})$ amount by the finite domain size. It follows that the stable localized states are found well within the expected regime $R_c < R < R^*$. As a result when R is increased outside the pinning region the behaviour remains simple: the bounding fronts depin, and new rolls nucleate as the fronts move apart, ultimately filling the domain with a periodic SOC state (figure 3*b*). In contrast in He^3–He^4 mixtures the conduction region between adjacent convectons fills with waves as R increases, as would be expected to occur once $R > R^*$ (Batiste & Knobloch 2005*a*, *b*).

5. Discussion and conclusions

In this paper we have examined the origin and structure of spatially localized steady convection in binary-fluid mixtures heated from below. We have used realistic boundary conditions and the parameter values used by Kolodner *et al.* (1990) in their experiments on dispersive chaos. We have seen that past the primary Hopf bifurcation the system settles into a state of dispersive chaos, much as in the experiments. This state is characterized by repeated growth and collapse of spatially localized structures (Kaplan, Kuznetsov & Steinberg 1994). We have seen that with increasing Rayleigh number the character of this state changes with the occasional formation of localized but almost stationary structures, much as observed by Kolodner *et al.* (1995) for slightly different parameter values. Our computations indicate that the localized steady states we have called convectons emerge from this state. Although branch-following techniques indicate that the convectons appear via saddle-node bifurcations little or no hysteresis has been observed in this transition.

We have seen that the convectons are organized into a pair of branches that snake towards the spatially periodic SOC state. As this occurs the convectons add rolls in a pairwise fashion, thereby becoming broader and broader. We have attributed this behaviour to the presence of a pinning interval in the Rayleigh number characterized by fronts separating the conduction and convection states, that are locked to the latter. Although we have not studied the stability of these states in detail we have confirmed via time-dependent integration the existence of multiple coexisting stable convectons within the pinning region. This multiplicity of states has thus far not been seen in experiments, possibly because self-trapping (Riecke 1992) precludes a change in the convecton size in any given experiment. The experiments do reveal, however, convectons of increasing width with increasing Rayleigh number (Kolodner 1993; Kolodner *et al.* 1995), presumably reflecting changes in the basin of attraction of the different convecton states. This in turn may be due to the ability of more vigorous convection to excavate a broader trough in the concentration distribution.

This work was supported in part by DGICYT under grant BMF2003-00657, AGAUR grant 2005SGR-00024 and by the National Science Foundation under grant DMS-0305968. We are grateful to J. Burke and A. Champneys for helpful discussions.

REFERENCES

Balmforth, N. J. 1995 Solitary waves and homoclinic orbits. *Annu. Rev. Fluid Mech.* **27**, 335–373.

Barten, W., Lücke, M., Kamps, M. & Schmitz, R. 1995 Convection in binary mixtures. II. Localized traveling waves. *Phys. Rev.* E **51**, 5662–5680.

Batiste, O. & Knobloch, E. 2005*a* Simulations of oscillatory convection in ^{3}He-^{4}He mixtures in moderate aspect ratio containers. *Phys. Fluids* **17**, 064102.

Batiste, O. & Knobloch, E. 2005*b* Simulations of localized states of stationary convection in ^{3}He-^{4}He mixtures. *Phys. Rev. Lett.* **95**, 244501.

Batiste, O., Knobloch, E., Mercader, I. & Net, M. 2001 Simulations of oscillatory binary fluid convection in large aspect ratio containers. *Phys. Rev.* E **65**, 016303.

Bensimon, D., Shraiman, B. I. & Croquette, V. 1988 Nonadiabatic effects in convection. *Phys. Rev.* A **38**, 5461–5464.

Blanchflower, S. 1999 Magnetohydrodynamic convectons. *Phys. Lett.* A **261**, 74–81.

Blanchflower, S. & Weiss, N. 2002 Three-dimensional magnetohydrodynamic convectons. *Phys. Lett.* A **294**, 297–303.

Burke, J. & Knobloch, E. 2006 Localized states in the generalized Swift-Hohenberg equation. *Phys. Rev.* E (in press).

Champneys, A. R. 1998 Homoclinic orbits in reversible systems and their applications in mechanics, fluids and optics. *Physica* D **112**, 158–186.

Coullet, P., Riera, C. & Tresser, C. 2000 Stable static localized structures in one dimension. *Phys. Rev. Lett.* **84**, 3069–3072.

Fauve, S. & Thual, O. 1990 Solitary waves generated by subcritical instabilities in dissipative systems. *Phys. Rev. Lett.* **64**, 282–284.

Glazier, J. A., Kolodner, P. & Williams, H. 1991 Dispersive chaos. *J. Stat. Phys.* **64**, 945–960.

Huerre, P. & Monkewitz, P. A. 1990 Local and global instabilities in spatially developing flows. *Annu. Rev. Fluid Mech.* **22**, 473–537.

Hugues, S. & Randriamampianina, A. 1998 An improved projection scheme applied to pseudospectral method for the incompressible Navier-Stokes equations. *Intl J. Numer. Meth. Fluids* **28**, 501–521.

Hunt, G. W., Peletier, M. A., Champneys, A. R., Woods, P. D., Ahmer Wadee, M., Budd, C. J. & Lord, G. J. 2000 Cellular buckling in long structures. *Nonlinear Dyn.* **21**, 3–29.

Kaplan, E., Kuznetsov, E. & Steinberg, V. 1994 Burst and collapse in traveling-wave convection of a binary fluid. *Phys. Rev.* E **50**, 3712–3722.

Knobloch, E. 1986 Oscillatory convection in binary mixtures. *Phys. Rev.* A **34**, 1538–1549.

Kolodner, P. 1993 Coexisting traveling waves and steady rolls in binary-fluid convection. *Phys. Rev.* E **48**, R665–668.

Kolodner, P., Glazier, J. A. & Williams, H. 1990 Dispersive chaos in one-dimensional traveling-wave convection. *Phys. Rev. Lett.* **65**, 1579–1582.

Kolodner, P., Slimani, S., Aubry, N. & Lima, R. 1995 Characterization of dispersive chaos and related states of binary-fluid convection. *Physica* D **85**, 165–224.

Kolodner, P., Surko, C. M. & Williams, H. 1989 Dynamics of traveling waves near the onset of convection in binary fluid mixtures. *Physica* D **37**, 319–333.

Lee, K. J., McCormick, W. D., Pearson, J. E. & Swinney, H. L. 1994 Experimental observation of self-replicating spots in a reaction-diffusion system. *Nature* **369**, 215–218.

Lioubashevski, O., Hamiel, Y., Agnon, A., Reches, Z. & Fineberg, J. 1999 Oscillons and propagating solitary waves in a vertically vibrated colloidal suspension. *Phys. Rev. Lett.* **83**, 3190–3193.

Mamum, C. K. & Tuckerman, L. S. 1995 Asymmetry and Hopf bifurcation in spherical Couette flow. *Phys. Fluids* **7**, 80–91.

Mercader, I., Batiste, O. & Alonso, A. 2006 Continuation of travelling-wave solutions of the Navier-Stokes equations. *Intl J. Numer. Meth. Fluids* DOI:10.1002/fld.1196.

Pomeau, Y. 1986 Front motion, metastability and subcritical bifurcations in hydrodynamics. *Physica* D **23**, 3–11.

Richter, R. & Barashenkov, I. V. 2005 Two-dimensional solitons on the surface of magnetic fluids. *Phys. Rev. Lett.* **94**, 184503.

Riecke, H. 1992 Self-trapping of traveling-wave pulses in binary mixture convection. *Phys. Rev. Lett.* **68**, 301–304.

Spina, A., Toomre, J. & Knobloch, E. 1998 Confined states in large aspect ratio thermosolutal convection. *Phys. Rev.* E **57**, 524–545.

Steinberg, V., Fineberg, J., Moses, E. & Rehberg, I. 1989 Pattern selection and transition to turbulence in propagating waves. *Physica* D **37**, 359–383.

Umbanhowar, P. B., Melo, F. & Swinney, H. L. 1996 Localized excitations in a vertically vibrated granular layer. *Nature* **382**, 793–796.

Vladimirov, A. G., McSloy, J. M., Skryabin, D. V. & Firth, W. J. 2002 Two-dimensional clusters of solitary structures in driven optical cavities. *Phys. Rev.* E **65**, 046606.

Woodcraft, A. L., Lucas, P. G. J., Matley, R. G. & Wong, W. Y. T. 1999 Visualisation of convective flow patterns in liquid helium. *J. Low Temp. Phys.* **114**, 109–134.